

## LETTERS

### Effect of Pressure on the Vibronic Luminescence Spectrum of a *trans*-Dioxo Rhenium(V) Complex

John K. Grey,<sup>†</sup> Myriam Triest,<sup>‡</sup> Ian S. Butler,<sup>\*,†</sup> and Christian Reber<sup>\*,‡</sup>

McGill University, Department of Chemistry, 801 Sherbrooke St. West, Montreal, Quebec, H3A 2K6, Canada, and Université de Montréal, Département de Chimie, Montréal, Québec, H3C 3J7, Canada

Received: March 6, 2001; In Final Form: May 9, 2001

Luminescence spectra of *trans*-ReO<sub>2</sub>(tmen)<sub>2</sub>Cl (tmen = tetramethylethylenediamine, (H<sub>3</sub>C)<sub>2</sub>N(CH<sub>2</sub>)<sub>2</sub>N(CH<sub>3</sub>)<sub>2</sub>), show pressure-dependent vibronic structure involving the high-frequency O=Re=O stretching mode in the <sup>3</sup>E<sub>g</sub> → <sup>1</sup>A<sub>1g</sub> transition (*D*<sub>4h</sub> point group). Its frequency and the intensity distribution within the progression are both pressure dependent. The ground-state O=Re=O frequency increases from 868 cm<sup>-1</sup> at ambient pressure to 887 cm<sup>-1</sup> at 51 kbar. The influence of pressure on the shape and relative positions of the ground and emitting state potentials is determined.

#### Introduction

Luminescence spectra recorded at different pressures reveal important information on the electronic structure of a wide variety of solid materials.<sup>1-5</sup> Transition metal complexes are particularly attractive for such studies because their electronic states involve different equilibrium geometries and bonding characteristics, an ideal situation to explore pressure effects on electronic transitions in the visible spectral region. Typically, experimental observations based on pressure-tuned electronic spectra are reported as shifts in the band maxima to either lower or higher energy and changes in band envelopes. These pressure-induced spectroscopic changes are usually analyzed with purely electronic energy level diagrams,<sup>1-5</sup> most often with ligand-field states, an approach that is not sufficient to analyze effects such as bond length differences between the ground and excited states. Resolved vibronic structure is essential for a more detailed analysis, and many low-temperature, ambient pressure electronic spectra have been analyzed in detail.<sup>9-12,14</sup> The majority of the high-pressure studies have been carried out at room temperature

or at moderately low temperatures where the vibronic progressions underlying absorption or luminescence bands are broadened, and unresolved band envelopes are observed. Resolved vibronic structure has been reported in a few pressure studies on doped impurities, frozen solutions, and molecules in solid matrices with spectra dominated by electronic origins and very short progressions involving a vibrational mode.<sup>6,7</sup> Purely electronic effects, such as ground-state exchange splittings, have been determined as a function of external hydrostatic pressure in neat crystalline coordination compounds, again using transitions with weak or absent vibronic structure.<sup>8</sup>

We present a series of pressure-tuned luminescence spectra from *trans*-dioxo bis-(tetramethylethylenediamine)-rhenium(V) with a resolved long progression at room-temperature involving the Raman-active O=Re=O stretching mode. *trans*-Dioxo complexes of rhenium(V) show low-temperature absorption and luminescence spectra with well resolved vibronic structure at ambient pressure.<sup>9-12,14</sup> The O=Re=O vibrational frequencies are on the order of 900 cm<sup>-1</sup>, higher by more than a factor of 2 than the majority of metal-ligand stretching modes in coordination compounds. This high frequency leads to spectra that show resolved vibronic structure even at room temperature. The experimental energies and intensity distributions allow us

\* Authors for correspondence.

<sup>†</sup> McGill University.

<sup>‡</sup> Université de Montréal.

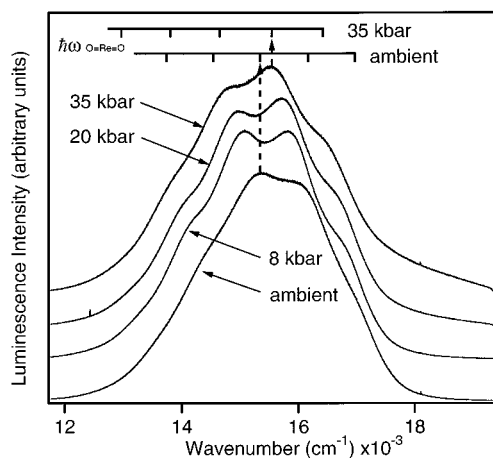


**Figure 1.** Luminescence spectra of *trans*-ReO<sub>2</sub>(tmen)<sub>2</sub>Cl as a function of pressure at room temperature. Spectra are offset along the ordinate for clarity.

to define the ground and emitting state potential energy surfaces along the normal coordinate of this vibrational mode. We calculate the luminescence spectra arising from these potentials and are able to characterize quantitatively the ground and emitting states as a function of pressure.

### Experimental Section

*trans*-ReO<sub>2</sub>(tmen)<sub>2</sub>Cl was synthesized and characterized using literature techniques.<sup>12–14</sup> To apply pressure to a crystalline sample, diamond-anvil cell (DAC) techniques were used. A small crystal of the title compound, a ruby chip, and Nujol were loaded into a gasketed DAC (300 μm diameter, High-Pressure Diamond Optics, Tucson, AZ) and the pressure was raised, in increments, up to 51 kbar. The R<sub>1</sub> peak of the ruby emission was used to calibrate pressures within ±10% of the actual pressure,<sup>15</sup> and Nujol was used as the pressure-transmitting medium. Luminescence spectra were collected with a Renishaw 3000 Raman microscope (20× objective), using the 514.5 nm line of an Ar<sup>+</sup> laser for excitation. The ruby chip was strategically placed so that the excitation laser could be focused to different regions of the sample area of the DAC. This allows us to obtain spectra from the sample with little or no interference from the intense ruby emission.

### Results and Discussion

Figure 1 shows pressure-tuned luminescence spectra from the title compound exhibiting resolved vibronic structure at room temperature. The emitting state for this and similar *trans*-dioxo complexes has been assigned, in idealized *D*<sub>4h</sub> point group symmetry, as a transition from a spin-orbit component of the <sup>3</sup>E<sub>g</sub> excited state to the <sup>1</sup>A<sub>1g</sub> ground state.<sup>9–12,14</sup> The electronic configurations for these two states are (d<sub>xz,yz</sub>)<sup>1</sup>(d<sub>xy</sub>)<sup>1</sup> and (d<sub>xy</sub>)<sup>2</sup>, respectively, with the *z* axis parallel to the O=Re=O double bonds. The energy range and maxima of the spectra in Figure 1 are also in good agreement with previously published low-temperature spectra at ambient pressure.<sup>12</sup> The dominant progression in the totally symmetric O=Re=O stretching mode is indicated in Figure 1 for the spectra recorded at ambient pressure and 35 kbar. The progression interval is approximately 870 cm<sup>-1</sup> at ambient pressure, corresponding to the totally symmetric O=Re=O stretching mode of the molecule observed in the ambient pressure Raman spectrum. As pressure increases to about 51 kbar, the frequency of this mode increases to 887 cm<sup>-1</sup>, indicating a higher Re=O force constant at high pressure.

**TABLE 1: Frequency of the Totally Symmetric O=Re=O Stretching Mode Determined from Raman Spectra as a Function of Pressure**

pressure (kbar)	$\hbar\omega_{\text{O=Re=O}}$ (cm <sup>-1</sup> )
ambient	868
6	869
11	870
25	877
31	880
37	883
46	886
51	887

Table 1 summarizes the experimental Raman frequencies, showing the effect of pressure on the order of a few tens of kilobars on the force constant of metal–ligand multiple bonds. To our knowledge, this is the first report on pressure-induced frequency changes for a metal–oxo double bond.

One of the most important features in this series of pressure-tuned luminescence spectra is the change of the intensity distribution within the vibronic pattern. The most intense component of the progression in Figure 1 shifts from the third to the second member at higher pressures, as indicated by the vertical dotted lines in Figure 1. In addition, the overall luminescence spectra show a noticeable red-shift as pressure increases, illustrated by the two lines with ticks at each vibronic transition throughout the progression.

We can understand these pressure-induced changes quantitatively by using time-dependent theory<sup>16,17</sup> with one-dimensional potential surfaces to calculate the luminescence spectrum at each pressure. As a first approximation, the harmonic potentials in eqs 1 and 2 are used for the ground and emitting states in the calculations.

$$E_{\text{GS}} = 1/2 \hbar\omega Q^2 \quad (1)$$

$$E_{\text{ES}} = 1/2 \hbar\omega(Q - \Delta Q)^2 + E_{00} \quad (2)$$

*Q* is the normal coordinate and  $\Delta Q$  is the offset between the ground and excited potential minima, in dimensionless units, as illustrated in Figure 3. *E*<sub>00</sub> is the energy of the origin of the emission and  $\hbar\omega$  is the frequency of vibration of the mode described by the normal coordinate *Q*; both quantities are in wavenumber units. We choose identical vibrational frequencies for both the initial and final states in our calculations. A lower value of 795 cm<sup>-1</sup>, determined from low-temperature absorption spectra,<sup>10,12</sup> does not lead to a significant improvement between observed and calculated spectra.

Figure 2 shows a comparison of experimental and calculated spectra, using eqs 1 and 2. The experimental luminescence band shape is not well described by a harmonic ground-state potential. The most significant deviations occur on the low energy side of the band. The agreement between the calculated spectrum and the experiment is improved significantly by using a Morse potential to represent the ground state. It is given by

$$E_{\text{GS}} = D \left( 1 - \exp \left\{ - \left( \frac{7.7588 \sqrt{\hbar\omega}}{D\sqrt{m}} \right) Q \right\} \right)^2 \quad (3)$$

where *D* is the dissociation energy, in cm<sup>-1</sup>, *m* is the mass of the mode in the ReO<sub>2</sub> fragment in g/mole, and  $\hbar\omega$  is the same vibrational frequency, in cm<sup>-1</sup>, as for the harmonic potential energy surfaces in eqs 1 and 2. The dissociation energy, *D*, was adjusted while holding  $\Delta Q$ , *E*<sub>00</sub>, and  $\hbar\omega$  close to the values used to define the simplest model based on harmonic potentials in eqs 1 and 2. This procedure leads to a significantly improved

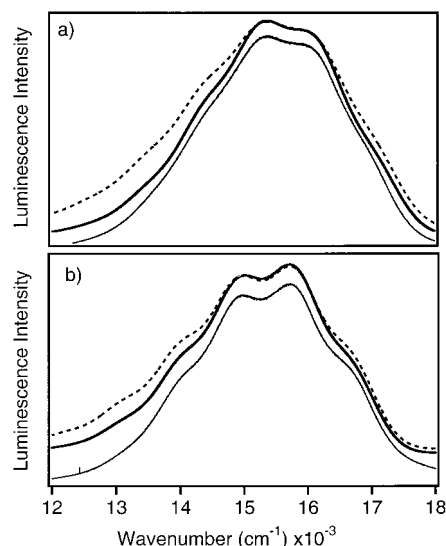


**Figure 2.** Comparison of experimental and calculated luminescence spectra at ambient pressure (a) and 35 kbar (b). The lowest trace in each panel denotes the experimental spectra. The calculated spectra obtained for harmonic and Morse ground-state potentials are shown as dashed and solid lines, respectively. The calculated spectra are offset from the experimental trace along the ordinate for clarity.

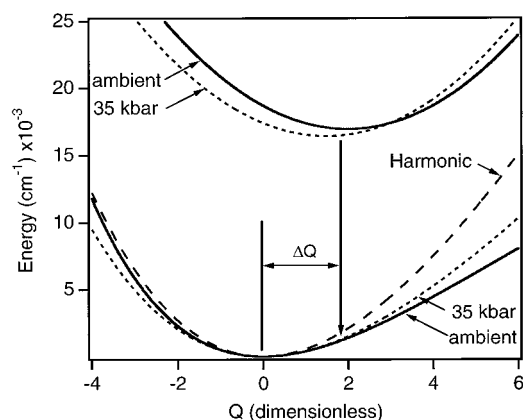


**Figure 3.** Potential energy surfaces for the ground and emitting states at ambient pressure (solid lines) and 35 kbar (dotted lines). The dashed line gives the harmonic ground-state potential surface at ambient pressure.

**TABLE 2: Parameters Determined from the Calculated Luminescence Spectra, as Illustrated in Figure 2 (all quantities defined in eqs 1–3)**

pressure (kbar)	$\hbar\omega_{\text{O=Re=O}}$ (cm <sup>-1</sup> )	$E_{00}$ (cm <sup>-1</sup> )	$\Delta Q$ (dimensionless)	$D$ (cm <sup>-1</sup> )
ambient	870	16 950	2.28	80 000
2	875	16 933	2.26	85 000
8	875	16 725	2.22	90 000
20	880	16 627	2.15	100 000
30	885	16 430	2.13	140 000
35	885	16 447	2.11	160 000

agreement between experimental and calculated spectra. Table 2 summarizes the parameters obtained from calculating the pressure-tuned luminescence spectra. The emission originates only from the lowest vibrational level of the excited state. Its eigenfunction is defined by the harmonic region around the potential minimum along  $Q$  and is not significantly affected by anharmonicity. We therefore use the harmonic excited-state potential described by eq 2. Figure 2 shows that the calculated spectra obtained with a Morse potential for the ground state

are in excellent agreement with the experimental data throughout the pressure range reported here.

The anharmonicity in the experimental spectra is due to avoided crossings between the potential surface of the  $^1A_{1g}$  ground state and excited states with the same symmetry.<sup>12,14</sup> The coupling between states flattens the ground-state potential surface at positive values of  $Q$ . The Morse potential is therefore a phenomenological description of the ground-state potential surface. The full account of this effect, established from low-temperature, ambient pressure spectra, involves two vibrational modes and three coupled electronic states.<sup>12</sup> These spectra show deviations from the Poisson band shape, which results from a harmonic ground-state potential, on the low energy side of the band, in qualitative agreement with the deviations illustrated in Figure 2. Our ambient temperature spectra are less resolved than the low-temperature luminescence spectra, showing only the high-frequency, totally symmetric O=Re=O stretching mode, and therefore we cannot fit all of the parameters required for the full model in ref 12. The Morse potential in eq 3, however, provides a good description with few adjustable parameters. This model explains the shape of the luminescence band envelope as a function of pressure. At pressures above 45 kbar, the vibronic structure washes out and the intensity of the emission drops significantly, indicating that nonradiative pathways dominate at higher pressures as a result of a strongly distorted excited state.

The use of Morse potentials to model the ground-state energy surface of the title compound yields the best fit to the experimental ambient pressure spectrum, significantly better than does the calculation using the harmonic ground-state potential in eq 1. This comparison is illustrated in Figure 2a. As pressure increases, the overall luminescence band shape is closer to the Poisson band shape expected for harmonic potential surfaces, as illustrated in Figure 2b, where the differences between the spectra calculated with harmonic and Morse potential surfaces are smaller than those in Figure 2a. By increasing the dissociation energy,  $D$ , of the Morse potential with increasing pressure, we can reproduce this behavior quite effectively. The red shift of the experimental spectra in Figure 1 leads to a decrease in  $E_{00}$ , as given in Table 2. The frequency,  $\hbar\omega$ , determined from the calculated luminescence spectra increases with pressure by the same amount as do the Raman frequencies given in Table 1. The precision of the frequencies in Table 2 is lower than for the Raman frequencies in Table 1, a difference due to the lower resolution of the luminescence spectra. The offset,  $\Delta Q$ , decreases with pressure, contributing to the change in the intensity distribution of the vibronic progression observed experimentally, allowing us to estimate the pressure-induced bond-length change of the Re=O double bonds. The decrease over the pressure range reported in Table 2 corresponds to a bond length change of 0.01 Å, on the same order as the variation of ambient pressure Re=O bond lengths for different ancillary ligands.<sup>18</sup>

The potential surfaces for the ground and excited states at low and high pressures are shown in Figure 3, illustrating the effect of pressure on the shapes of these surfaces. The red shift of the emission with increasing pressure is a consequence of both the decrease of the energy difference,  $E_{00}$ , between the lowest vibrational levels within the ground and emitting state potential surfaces and the smaller anharmonicity, corresponding to a higher dissociation energy,  $D$ , of the ground-state potential surface in eq 3. High-pressure pushes the ground-state surface in Figure 3 to higher energy in the normal-coordinate range of the luminescence maximum, indicated by the vertical arrow, an effect that causes the band envelope at high pressure to

resemble a Poisson band shape expected for a harmonic ground state potential. The change of the intensity distribution within the vibronic progression depends on two pressure-induced effects: first, the decrease of the offset,  $\Delta Q$ , between the minima of the potential curves with increasing pressure, and, second, the increase of the dissociation energy,  $D$ , with pressure. This latter effect is expected to dominate when the ground-state potential surface at ambient pressure is strongly anharmonic and becomes less important for complexes with a nearly harmonic ground-state potential surface at ambient pressure.

The deviation from an harmonic ground-state potential in the title complex is caused by coupling between the ground-state and emitting-state surfaces, and we therefore expect distinctly different pressure effects on the emission spectra of *trans*-dioxo complexes with higher or lower energy luminescence than shown in Figure 1. Our results show that the spectroscopic effects of coupling between electronic states, even if they are separated by more than  $10^4 \text{ cm}^{-1}$ , can be better understood by pressure-tuning methods applied to spectra with resolved vibronic structure.

**Acknowledgment.** This work has been made possible by research grants from the Natural Sciences and Engineering Research Council (Canada).

## References and Notes

- (1) Drickamer, H. G. In *Solids Under Pressure*, Paul, W.; Warshauer, D., Eds.; McGraw: New York, 1963; p 357.
- (2) Drickamer, H. G.; Frank, C. W. *Electronic Transitions and the High-Pressure Chemistry and Physics of Solids*; Chapman and Hall: London, 1973.
- (3) Schäffer, C. E.; Lang, J. M.; Drickamer, H. G. *Inorg. Chem.* **1996**, *35*, 5072.
- (4) Bray, K. L.; Drickamer, H. G.; Schmitt, E. A.; Hendrickson, D. N. *J. Am. Chem. Soc.* **1989**, *111*, 2849.
- (5) Ferraro, J. R.; Basile, L. J.; Sacconi, L. *Inorg. Chim. Acta* **1979**, *35*, L317.
- (6) Kenney, J. W., III; Clymire, J. W.; Agnew, S. F. *J. Am. Chem. Soc.* **1995**, *117*, 1645.
- (7) Yersin, H.; Trümbach, D.; Wiedenhofer, H. *Inorg. Chem.* **1999**, *38*, 1411.
- (8) Riesen, H.; Güdel, H. U. *J. Chem. Phys.* **1987**, *87*, 3166.
- (9) Winkler, J. R.; Gray, H. B. *J. Am. Chem. Soc.* **1983**, *105*, 1373.
- (10) Winkler, J. R.; Gray, H. B. *Inorg. Chem.* **1985**, *24*, 346.
- (11) Miskowski, V. M.; Gray, H. B.; Hopkins, M. D. In *Advances in Transition Metal Coordinate Chemistry*; Che, C.-M., Yam, V. W.-W., Eds; JAI Press: Greenwich, CT, 1996; p 159.
- (12) Savoie, C.; Reber, C. *J. Am. Chem. Soc.* **2000**, *122*, 844.
- (13) Lock, C. J. L.; Turner, G. *Acta Crystallogr.* **1978**, *B34*, 923.
- (14) Savoie, C.; Reber, C. *Coord. Chem. Rev.* **1998**, *171*, 387.
- (15) Piermarini, G. J.; Block, S.; Barnett, J. D.; Forman, R. A. *J. Appl. Phys.* **1975**, *46*, 2774.
- (16) Heller, E. J. *Acc. Chem. Res.* **1981**, *14*, 368.
- (17) Zink, J. I.; Kim Shin, K.-S. *Advanced Photochemistry*; Volman, D. H., Hammond, G. S., Neckers, D. C., Eds.; Wiley: New York, 1991; p 119.
- (18) Mayer, J. M. *Inorg. Chem.* **1988**, *27*, 3899.